The *AKARI* Mid-IR All-Sky Diffuse Maps: Lessons Learned for *SPICA*

Toru Kondo,[1] Daisuke Ishihara,[1] Hidehiro Kaneda,[1] Shinki Oyabu,[1] Tomoya Amatsutsu,[1] Satoshi Suzuki,[1] Mitsuyoshi Yamagishi,[1] Takafumi Ootsubo,[2] Takashi Onaka,[3] Ryou Ohsawa,[3] and Fumihiko Usui[4,3]

[1]*Graduate School of Science, Nagoya University, Japan*
[2]*Department of Astronomy, Tohoku University, Japan*
[3]*Astronomical Institute, The University of Tokyo, Japan*
[4]*Institute of Space and Astronautical Science, JAXA, Japan*

ABSTRACT

We are creating all-sky diffuse maps from the *AKARI* 9 and 18 μm band survey data. In particular, the 9 μm map is a unique resource as an all-sky tracer of polycyclic aromatic hydrocarbons. Original data include artifacts, such as the scattered light from the moon. In addition, the zodiacal light is a dominant component compared to the Galactic interstellar emission in the mid-IR. In order to correct these artifacts and remove the zodiacal light, we have carried out special analyses. As a result, we have obtained accurately-calibrated all-sky maps and learned technical lessons for *SPICA*.

1. INTRODUCTION

AKARI carried out mid-IR all-sky surveys in the 9 and 18 μm bands. The 9 μm map is crucial to investigate the all-sky distribution of polycyclic aromatic hydrocarbons (PAHs), while the 18 μm map is useful to trace hot dust grains. However, original data include artifacts, such as the scattered light from the moon. Figure 1 *Top* shows an example of the *AKARI* 9 μm map around the Galactic center affected by these artifacts. In addition to these artifacts, the zodiacal light is a dominant component in the mid-IR. We have to remove the zodiacal light from the maps to obtain the Galactic diffuse maps. It has been physically modeled in past studies (e.g., Kelsall et al. 1998), however, there remains discrepancy between the observational result and model prediction, which is still larger than Galactic cirrus emission at high galactic latitudes (Kondo 2013). In order to obtain accurate mid-IR Galactic diffuse maps, we have carried out special analyses.

2. DATA REDUCTION AND RESULTS

2.1. Removal of the Scattered Light from the Moon

We found that the observational data are strongly affected by the scattered light from the moon, even if the moon is about 40 degrees away from the field of view (Mouri 2012). We therefore evaluated the pattern of the scattered light from the moon in the detector array coordinates with the moon in the center (Figure 2). As a result, we obtain the pattern which is asymmetrical with respect to the moon position with spider-like structures. Thus, the intensity of the scattered light cannot be estimated as a function of the moon avoidance. We also find that the scattered light is distributed over 40 degrees away from the moon. Because this pattern is stable from season to season, we establish the method to remove the scattered light component from the maps. Figure 1 *Bottom* shows the 9 μm map around the Galactic center after removing the scattered light from the moon.

2.2. Removal of the Zodiacal Light

We have obtained the maps in which we corrected the artifacts, as shown in Figure 1 *Bottom*. Yet, the zodiacal light is a dominant foreground emission compared to the Galactic diffuse emission as shown in Figure 3 *Left*. In the standard zodiacal light model, the interplanetary dust cloud is composed of three components: the smooth cloud, the dust bands, and the mean-motion-resonance (MMR) component (Kelsall et al. 1998). In past studies, the emissivities of these three components were determined by the zodiacal light model fitting using the data of seasonal variations of the zodiacal light (Kelsall et al. 1998; Pyo et al. 2010).

On the other hand, we divide the MMR component into the circumsolar ring and the trailing blob, and carry out the model fitting simultaneously using all the seasonal data. As a result, we obtain the emissivity of each component shown in Table 1,where we also show the emissivity determined by the *COBE*/DIRBE 12 μm band (Kelsall et al. 1998) for comparison. We find that the emissivities of the MMR component (especially the trailing blob component) in the 9 μm band are higher than those in the 12 μm band, while the emissivity of the smooth cloud is similar in both bands. On the contrary, the emissivity of the dust bands in the 9 μm band is considerably lower than that in the 12 μm band. After these modifications of the emissivity parameters, we successfully reduce the intensity of the residual component down to 2 % of the zodiacal light component at the ecliptic plane, which is compared with 6 % in the past study (Kelsall et al. 1998). Figure 3 *Right* shows the result of the removal of the zodiacal light in the 9 μm band.

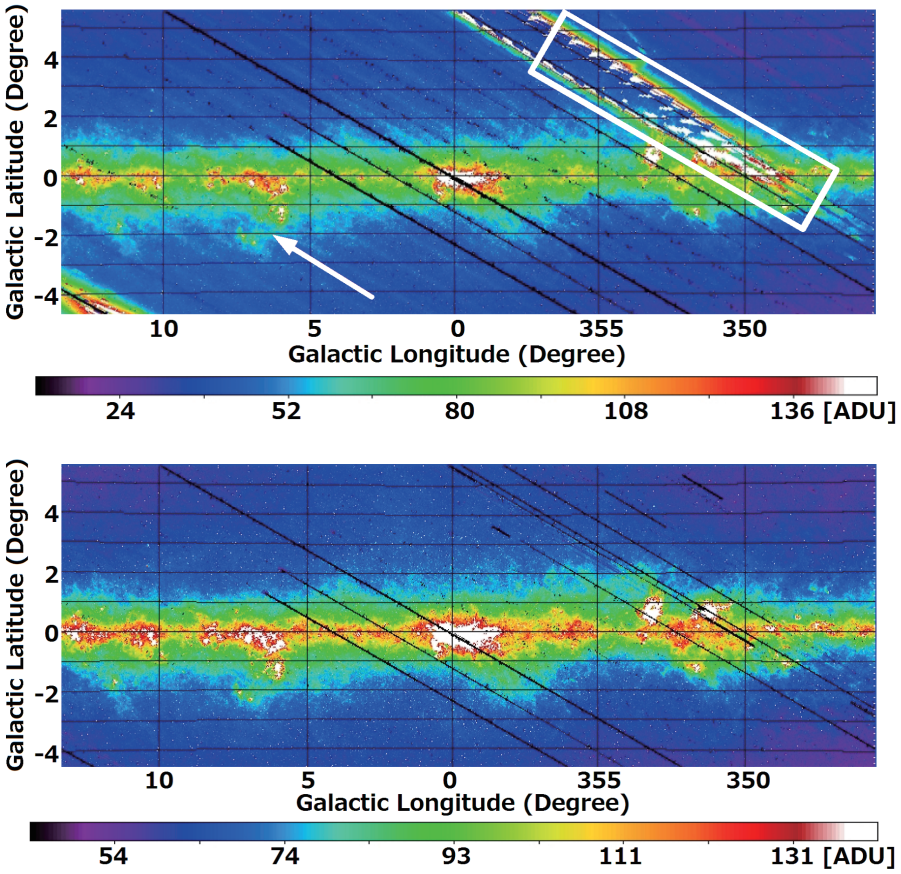

Figure 1. *Top*: *AKARI* 9 μm map around the Galactic center of an area of about 30 deg $\times$10 deg. The white box and the white arrow indicate the scattered light from the moon and the scan direction, respectively. The stripes parallel to the scan direction are ionizing radiation effects (The detail appears in Mouri et al. (2011)). *Bottom*: Same data as the top panel, but after removing the scattered light from the moon and the ionizing radiation effects.

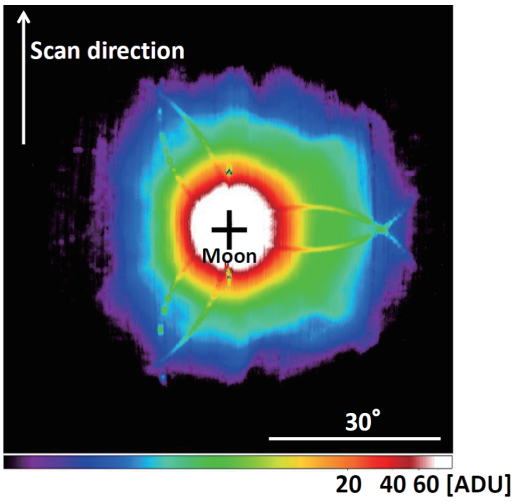

Figure 2. Pattern of the scattered light from the moon in the 9 μm band in the detector array coordinates. The moon is located in the center.

3. LESSONS LEARNED FOR *SPICA*

We have learned technical lessons for *SPICA* through the correction of the scattered light from the moon and the removal of the zodiacal light. *SPICA* will suffer stray light of objects fainter than the moon (e.g., asteroids, bright stars) because the sensitivity of *SPICA* is higher than that of *AKARI*. We have identified critical paths of the scattered light from the moon into the telescope, investigating the structure of the telescope baffle and the pattern of the scattered light shown in

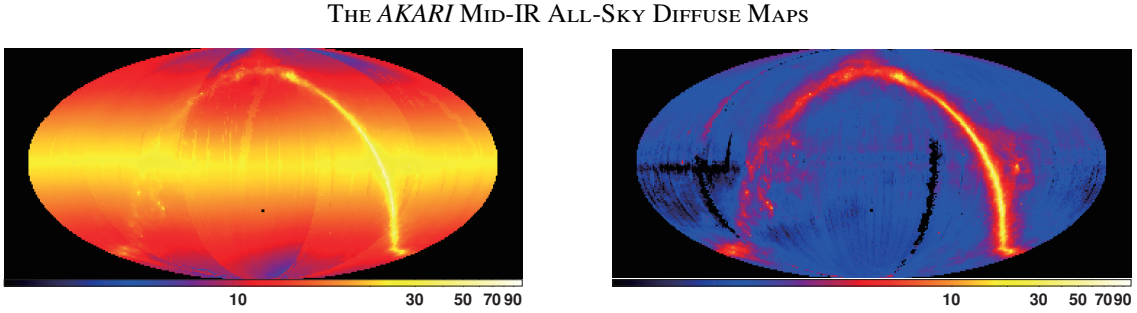

Figure 3. The 9 μm all-sky maps in the ecliptic coordinates before (*left*) and after (*right*) removing the zodiacal light. The units of the color scales are given in MJy sr^{-1}.

Table 1. Emissivity modification factors.

Wavelength	Smooth cloud	Dust bands	Ring	Blob
9 μm (present study)	1.084 ± 0.002	0.31 ± 0.04	1.55 ± 0.04	2.80 ± 0.02
12 μm (Kelsall et al. 1998)	0.958 ± 0.003	1.0 ± 0.2	1.06 ± 0.09	

Figure 2. We feed back the information to the optical design of the baffle of *SPICA*. For the zodiacal light, we improve the model parameters to explain the *AKARI* data. The new zodiacal light model will be useful for observation planning and data reduction of *SPICA*.

4. SUMMARY

The *AKARI* 9 μm map is a unique resource as an all-sky PAH tracer. In order to create accurately calibrated maps, we have carried out special data analyses, such as correction of the scattered light from the moon and removal of the zodiacal light. As a result, we have learned technical lessons for *SPICA* through these analyses.

We thank all the members of the *AKARI* project. T.K. is financially supported by Grants-in-Aid for JSPS Fellows No. 25-2536.

REFERENCES

Kelsall, T., et al. 1998, ApJ, 508, 44
Kondo, T. 2013, Master's thesis, Nagoya University
Mouri, A. 2012, Master's thesis, Nagoya University
Mouri, A., et al. 2011, PASP, 123, 561
Pyo, J., et al. 2010, A&A, 523, A53